Fully Tunable $LiNbO_3$ Ring Resonator Cavity for Frequency Comb Generator (FCG)

A. Kaplan, A. Greenblatt, G. Harston, P. S. Cho, Y. Achiam and I. Shpantzer
CeLight Inc. 12200 Tech Road, suite 200, Silver Spring, MD, 20904, akaplan@celight.com

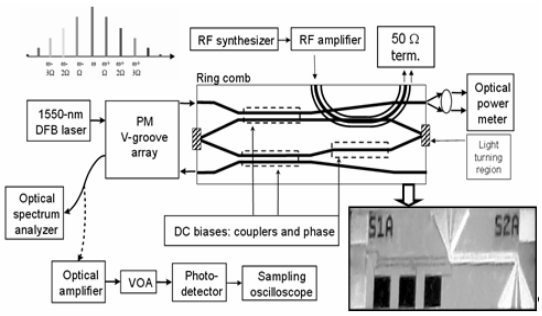

Fig. 1: Ring resonator optical comb schematic view and test setup. Inlay with actual device picture is shown.

Abstract: *A novel $LiNbO_3$ ring resonator cavity is developed for the tunable optical frequency comb generation. Such device enables a high frequency RF modulation of the optical field with independent tuning of the resonator add/drop coupling and phase. The modeling of the integrated ring FCG, fabrication and some experimental results are described.*

Introduction

Using an electro-optical phase modulator placed into a resonant cavity is the most direct method of producing a frequency comb that can be also viewed as an optical pulse generator for use, for example, in optical coherent sensing and tomography [1-2]. The modulation frequency should consist of a multiple number of the optical cavity FSR (an integer number of fringe separations) thus efficiently producing a comb by resonantly enhancing the modulation sidebands. High modulation frequency and electro-optical efficiency can provide a relatively broad resulting spectrum. The high bandwidth can be achieved by implementing traveling wave electrodes so that the electrical field co-propagates with the optical field in the $LiNbO_3$ substrate.

Integrated Ring FCG

In practice, a reliable wide spectral coverage (narrow pulse-train) requires high accuracy stable optical sources along with the well-controlled phase and cavity input/output coupling.

There are some drawbacks limiting the performance of the conventional FCG [3], such as suppression of the total sidebands power caused by increasing the mirror refractivity to increase the relative power transferred to the high order sidebands. By increasing the finesse (and/or modulating index) the pulse-width is narrowed while the peak power remains the same, thus decreasing the sidebands total power (average). Another difficulty is a small cavity size (1-2cm) (needed for a desired bandwidth) limits the modulating index and overall electro-optical design flexibility. With these issues in mind, a new type of ring-resonator FCG with tunable add/drop coupling was developed [3]. The problem of the high radiative bend losses associated with the weakly-guiding $LiNbO_3$ ring cavity was addressed by developing relatively low-loss light-reflective regions that helped to overcome the minimal limit for the cavity circumference needed for a reasonably large bandwidth. A schematic view of the ring-cavity OFG and photograph of the actual device are shown Fig. 1.

The analysis of the passive (without RF modulation) ring resonator with the tunable add/drop coupling is described elsewhere [4] for several types of couplers. It was shown that for a realistic lossy cavity the optimal, generally non-identical, add/drop coupling values can be defined and adjusted accordingly via the independent electro-optical perturbations of the couplers and resonator phase. Fig. 2 shows the quality/contrast optimization of such a tunable ring resonator.

3. Ring FCG experiment

The test setup is shown in Fig. 1. Two FCG cavity lengths of ~2.25 and ~4.5 cm were fabricated, both supporting ~6 and ~12 GHz modulating frequencies. An external 1550-nm DFB laser source was coupled into one of the bus waveguides of the ring resonator via a V-groove PM fiber array. The thru port of the comb output on the right side was directed to an optical power head using a focusing lens while the reflected port was fiber-coupled via the same V-groove array. RF and DC probes were applied to the traveling-wave, phase, and coupler electrodes of the device. Optical signal from the reflected port was monitored using an optical power meter, optical spectrum analyzer (OSA), and a 30-GHz sampling oscilloscope for

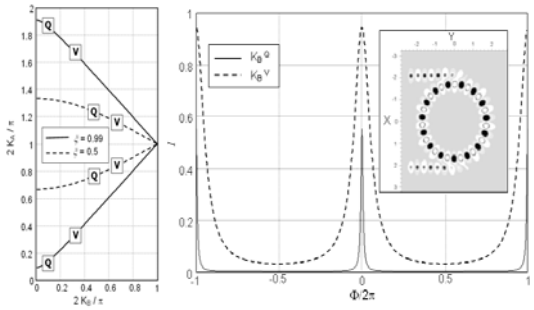

Fig. 2: a) Resonant coupling diagram. Marks indicate the coupling values for the maximum resonator quality Q or contrast V given for two values of cavity losses (1-ξ).
b) Q- and V- resonator response optimization by passive design or by an external tuning; for ξ=0.99.

monitoring of pulse train. RF signal was applied to the traveling-wave electrodes to produce phase-modulated output. Resonance of the comb was determined by an on-resonance (close to integer multiple of the FSR) and off-resonance RF drive frequency.

For high-resolution passive transmission spectrum extinction ratio measurement, the DFB laser was replaced with a wavelength-tunable laser and an optical power meter was used to measure the optical power at

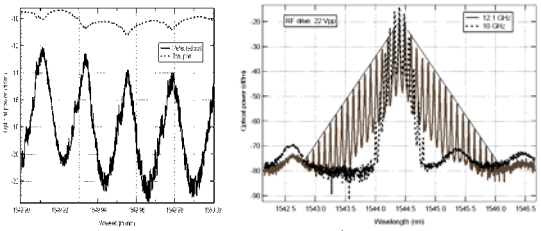

Fig. 3: a) Spectral scan of the reflected and thru ports of the ring OFG output. b) Optical spectrum of the reflected port with of 12.1GHz drive frequency (near resonance) and 10GHz (off-resonance). Resolution bandwidth: 0.01nm.

the reflected output port of the ring FCG device. The power (extinction) ratio recorded by the spectral scan is a function of the resonator finesse. Alternatively, a fixed wavelength laser can be used while the phase voltage of the comb device is swept to determine its spectral response. Fig. 3a shows a typical spectral scan for particular ring FCG. Both reflected and transmitted optical powers versus wavelength are shown. The measured FSR was about 2.84 GHz and the extinction ratio for the reflected port output is about 8dB.

Fig. 3b shows OSA spectral output from the reflected port of FCG driven at 12.1 and 10GHz (on- and off-resonance, respectively). The resolution bandwidth of the OSA was 0.01nm. The RF drive voltage was about 22 V peak-to-peak. The slope of the comb envelope was estimated to be about -0.28 dB/GHz at resonance. With off-resonance drive at 10 GHz the number of wavelengths reduced drastically. The temporal output of the ring comb device was monitored using a sampling oscilloscope as shown in Fig. 1. The repetition rate of the pulse train varies between 12.1 and 24.2 GHz (on- and off-resonance, respectively). An estimated finesse and modulation index was about 3.62 and 2.2, respectively. Several control loops for maintaining resonant FCG were suggested.

Active Control for FCG

One of the proposed control loops is based on a counter-propagating controlling laser, derived from the same external injected laser but launched counter-propagating to the RF traveling wave through the FCG as shown in Fig. 4. The clockwise-propagating control laser does not experience instantaneous phase modulation but only an average phase shift. The optical power of the control laser from the comb output can be used directly as a feedback signal to indicate whether or not the comb is in resonance. A device was tested using the counter-propagating configuration to check the residual phase modulation. The test setup is similar to that shown in Fig.1 except that the RF signal is applied to the other end of the traveling-wave electrode so that it travels opposite to the optical wave. Typical results are shown in Fig 5. RF peak-to-peak drive voltage was 8.69V at 12.1GHz. One can see that in either case the sideband-to-carrier power ratio is significantly reduced compared with the co-propagating case. The existence of sidebands at all in the counter-propagating case is likely due to reflections at the various waveguide interfaces. Due to multiple reflections a portion of the reflected control laser may co-propagate with the RF signal, experiencing instantaneous phase modulation, and later recombine with the counter-propagating laser.

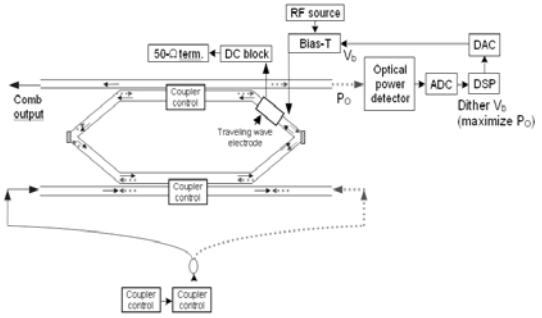

Fig. 4: Proposed resonant control for the ring comb based on monitoring of the output optical power of a clockwise laser shown in dashed line (feedback signal). The comb output is represented by the counter-clockwise arrow.

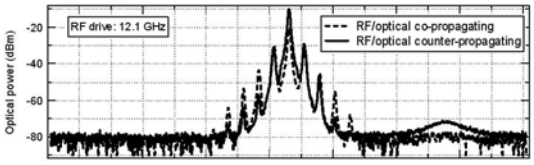

Fig. 5: FCG output spectra for 12.1GHz obtained with co- and counter-propagating optical and RF wave.

A feedback control loop based on monitoring the optical output of the comb device was also considered. When the comb device is driven by a sinusoidal RF signal at a modulation frequency of f_m an optical pulse train output with a repetition rate of $2f_m$ is expected when resonant conditions are met as shown in Fig. 6. This requires f_m to be precisely set according to the FSR of the comb resonator and also the injection laser optical frequency must be an integer multiple of the FSR or align to one of the resonant frequencies of the comb device.

One can obtain useful information on the operation status of the comb device by monitoring its output such as the average optical power (*Po*) and the RF power at *fm* (*VRF*) of the pulse train. The RF power of the pulse train can be obtained by using a photodetector with a bandwidth around *fm* followed by a RF detector to extract the RF power at *fm*.

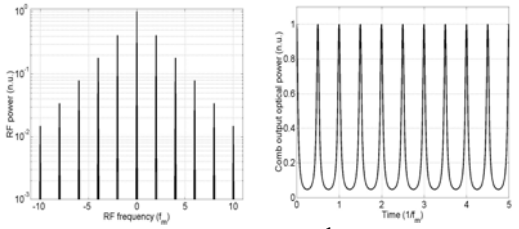

a. b.

Fig. 6: a) Simulated pulse output of the optical comb biased at resonance. Note the pulse repetition rate is twice the modulation frequency, f_m. b) RF power spectrum of the pulse train shown on the left. Note the absence of odd harmonics of f_m.

Fig. 7 shows a typical plot of the calculated *Po* and *VRF* versus the comb phase bias based on a comb resonator model [2]. The comb phase bias changes the resonant frequencies which affects the resonant condition. In Fig. 7, resonance occurs at comb phase bias of 0 or integer multiples of p. Both *Po* and *VRF* approach to their respective minimum values at resonance. However, *Po* and *VRF* also reach minimum values at off-resonance (e.g., phase=π/2). Therefore, a resonance control algorithm based on minimizing *Po* and *VRF* may or may not converge to resonance depending on the initial phase bias. In order to ensure convergent to resonance regardless of the initial phase bias, the control algorithm must first adjust the comb bias to maximize *Po*.

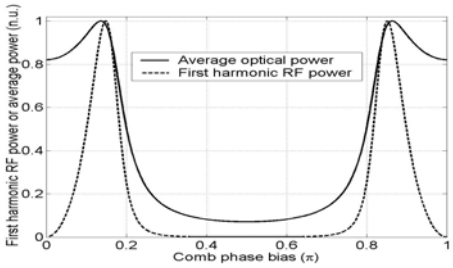

Fig. 7: Average optical power and RF power of the f_m first harmonic or V_{RF} versus phase bias. Resonance corresponds to comb phase bias of zero or integer multiples of π.

Once *Po* reaches maximum, the comb bias must be varied to minimize *VRF*. Note that if the modulation index is high, the relative phase bias position where maximum of *Po* and *VRF* are located may be interchanged. In this case, the algorithm should be modified so that *VRF* be maximized first followed by minimization of *Po*.

Experiments were conducted to verify the operation of the resonant control loop and also validate the performance of the variable ring comb. Fig. 8 shows the pulse waveforms of the ring comb output displayed on the sampling oscilloscope with and without the resonant control loop running. The sampling oscilloscope was set to infinite persistent mode so that drift and fluctuations of the comb output can be accumulated and recorded. Note that the pulse waveforms shown in the figures are limited by the detection bandwidth (40GHz) of the oscilloscope. With the control loop running, one can see from Fig. 8 that the ring comb device is maintained at resonance with a stable output pulse train at a repetition rate of about 24.4 GHz or 2*fm*. On the other hand, without the control loop the comb device seems to fluctuate randomly in and out of resonance causing the output pulse pattern to drift in time. As a result, no stable pulse train at 2*fm* was observed. The fluctuation can be attributed to variation of the injection laser optical frequency and environmental-induced perturbations on the refractive index of the LN waveguide of the comb device.

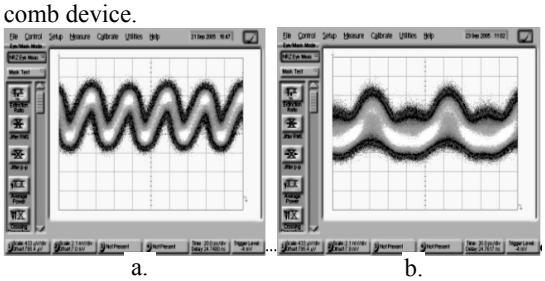

a. b.

Fig. 8: Pulse train of ring comb output with (a) and without (b) resonant control. Injection laser wavelength: 1544nm. The comb is driven at 12.2GHz. a)- pulse repetition rate is 24.4GHz. Detection bandwidth: 40GHz. Infinite persistent mode ~ 2 minutes. Horizontal scale: 20ps/div.

Conclusions

A novel fully tunable, $LiNbO_3$-integrated weak-guiding ring FCG device was developed. This device potentially overcomes the limitations of integrated $LiNbO_3$ Fabry-Perot cavities and existing ring cavities with limited coupling tunability. Preliminary experimental results are consistent with the simulation results. Current and future development includes the add/drop adjustment optimization, cavity losses minimization, and improved resonant control scheme that utilizes both available optical and electrical outputs for a more robust and stable performance.

$LiNbO_3$-based electro-optical ring resonators with autonomous input/output coupling ratios and phase tuning may become promising components for a variaty of applications such as FCG, channel add-drop filters, sensors, chromatic dispersion compensators, optical delay lines, and Er-doped cavities for loss compensation, to mention a few.

Acknowledgments

This work was partially supported by Contract DMEA H94003-04-D-0004.

References

1 M. Kourogi et al, IEEE J. Quantum Electron., vol.29, No.10, pp. 2693, 1993.

2 Fixed and Variable Optical Grid Comb Design Document, CeLight Inc., Technical Report Provided to Northrop Grumman for Secure Digital Coherent Optical Communications (SDCOC). Defense Microelectronics Activity (DMEA), 2005.

3 A. Kaplan et al., Coherent Optical Technologies and Application Topical Meeting, OSA Technical Digest, Whistler Canada, 2006, paper CFC3.

4 A. Kaplan, IEEE Selected Topics in Quantum Electronics, Vol.12, pp. 86-95, 2006.